2D Hemodynamic Imaging

Riku Saarenheimo
Master's Thesis
Science and Engineering
Department of Applied Physics
University of Eastern Finland, Kuopio Campus
June 17, 2012

University of Eastern Finland, Department of Science and Forestry
Science and Engineering / Engineering Physics
Riku Saarenheimo: 2D Hemodynamic Imaging
Master's Thesis
Instructors: Prof. Alexei Kamshilin (PhD), Ervin Nippolainen (DSc)
May 2012

Keywords: hemodynamic imaging, blood pulsation, pulse oximetry, pulse plethysmography, synchroneous detection

Hemodynamic imaging is a novel imaging system for visualizing blood pulsations in living tissue. It has some similarities with modern pulse oximetry and pulse plethysmography methods, but some differences set it apart from them. The system is based on illuminating the studied subject and detecting minute variations in the intensity of light scattered from the tissue, caused by changes in local blood volume as the blood vessels and capillaries pulsate due to pressure waves caused by the heart beats. A method of synchroneous detection is used to amplify the variations taking place with the frequency of the heart beats to greatly improve signal-to-noise ratio and make it possible to create a complex-valued matrix that accurately describes the amplitude and relative phase of the pulsations in different parts of the measured area.

The system can be used for clinical experiments to inspect and monitor the blood pulsations in patients with diseases or other conditions that cause abnormalities in the flow of blood. It can be used as a diagnostic tool to detect such conditions, or to monitor the patients for example to investigate the effects of treatments. The technology shows great promise in the field of medical science, and new possible applications are still arising.

For this thesis, we conducted a series of experiments to determine the performance of the system under different wavelengths of illumination ranging from 460 to 920 nm. The results showed that while the system gave the strongest response at 521 and 811 nm, all wavelengths provided a detectable signal. This information makes it possible to apply the system for an even wider range of applications, such as pulse oximetric imaging. The information also helps to develop the system and improve its performance in the future.

In addition to these measurements, this thesis also gives a brief introduction to the optical properties of skin and some methods of optical analysis, and describe the structure, operation and data analysis process of the system.

Contents

1 Introduction

Skin is the largest organ in the human body, and it has properties ranging from chemical resistance to mechanical durability. It covers our bodies and protects us from the environment, still allowing necessary metabolic phenomenon to take place. Its structure is complex and hard to model, and it is the defining boundary element of our physical existence.[1]

There is a large interest in the study of physical, and specifically medical, properties of the skin. There are diseases related to skin that can affect its behaviour. For example, some diseases can cause changes in the pigmentation of skin, cause irritation or affect the optical properties of skin. These can be used to diagnose things such as lack of oxygen or the early stages of skin cancer.[1, 2, 3]

There are various different methods and devices for clinical analysis of skin, many of which are in everyday use in modern hospitals. One example of such a device is the pulse oxymeter, a device which uses the minute changes of light absorbtion in the skin caused by the varying concentrations of oxygenated and deoxygenated haemoglobin to determine the oxygen saturation level in the blood[3]. It is a standard in modern medicine for monitoring the condition of patients.

It is known that the pulsations of the heart cause a pressure wave, which traverses along the blood vessels, slightly expanding and constricting them as it passes[4], and a method using the same principle as pulse oximetry called photoplethysmography, or optical volumetric measuring is also well known and used for monitoring the pulsations of blood. Photoplethysmographs (PPG) are currently commonly used to monitor the heart rate of patients in hospitals.[5]

While such methods are physically interesting and provide information for medical analysis and monitoring, they have two major limitations. Firstly, their signal is sensitive to disturbances caused by external effects, and secondly, they can only obtain information from a single point. A pulse oximeter, for example, is typically placed on the finger of the patient and measures the signal from light transmitted through the tissue. A slight movement of the finger or other external influences such as light or strong electric fields can affect the signal, and weakened blood flow for example due to hypothermia or shock can make measurements impossible.[6]

Attempts have been made to modify these methods to collect information from a larger area using 1D- or 2D-cameras in reflectance geometry, creating a larger field of view[7, 8]. The devices normally have more complex structures and are more sensitive to external and internal disturbances. The relative amplitude of the observed variations is so small that it makes direct analysis difficult, and the effects caused by disturbances such as movement or unstable illumination make it even more challenging.

Our research group became interested in this problem upon noticing small pulsations in the intensity signal measured from skin using an experimental 2D spectral camera with regular light emitting diodes as illuminators. Analyzing the information, we realized that by amplifying the variations in the intensity that were occurring with the frequency of the heartbeat we could greatly improve the performance of the system, to the extent that we were able to create a high-resolution animation showing the propagation of a cardiac pressure wave in the skin.[9]

Our system has since been refined, and we have begun clinical trials in various fields. Some possible applications can be found for example in migraine research, study on the effects of arthritis in peripheral circulation, and monitoring the condition of skin flaps. We are continuing to improve the system to increase its performance and applicability. Our aim is to develop it into a product that can be used for routine analysis in various medical fields. For further reference, we are proposing the tentative name of hemodynamic imaging for our method, as it is an imaging system that visualizes the dynamic nature of blood pulsation.

The aim of this thesis is to study the performance of the hemodynamic imaging system under different wavelengths of illumination in the visible and near-infrared diapason through a practical experiment. The contents of the thesis are an introduction to the anatomical and optical properties of skin and the phenomenon related with the signal formation in measurements, a brief introduction to some optical methods related to hemodynamic imaging, a description of the general and specific structure of the hemodynamic imaging system, explanation of the signal formation from captured images based on an example, and finally description of measurements and results, with in-depth discussion.

2 Interaction between light and skin

The optical properties of human skin are related to the anatomical properties of skin. The main phenomenon affecting the optical properties of skin are absorption and scattering[10]. Other phenomenon, such as photoluminescence, are also possible but as their effects are generally small they are not considered in this thesis.

In absorption, the energy of a photon is transferred to atoms or molecules in the sample, often in the form of heat, and a decrease in the number of photons can be observed. Scattering on the other hand can be simplified as a photon changing its direction, and sometimes also its wavelength, after interaction with the atoms or molecules. In this case the number of photons does not change.[16] The method of hemodynamic imaging focuses on detecting photons that enter the tissue and undergo multiple scatterings until they are back-scattered out of the tissue to the detector of a camera.

Another relevant term in investigating the interaction between light and skin is penetration depth, which is defined as the depth in the material at which the intensity of light is reduced to 1/e, or approximately 37%, of the original intensity due to absorption and scattering. In skin, this penetration depth is a function of the wavelength of light, and it is also affected by properties of the skin such as pigmentation, and the relative amount and oxygenation of blood. Penetration depth follows a gaussian distribution, and therefore a small number of photons will travel longer distances and are capable of providing information even from deeper within the tissue.[16]

In real measurements analyzing each photon separately, following its path and possible scatterings and absorption is impossible due to the vast number of photons and the complex structure of skin. It is possible to create models for this behaviour, which simplify the analysis.[17, 18] A typical solution is to find coefficients for absorption and scattering that can be used to describe the average behaviour of photons in different regions of skin. This thesis will not consider specific models for estimating the optical properties of skin with much detail, but some of their properties are discussed.

2.1 Anatomy of skin

Human skin is part of the integumentary system and it has many vital functions, such as protecting the body from external influences and damage, controlling body temperature by sweating and producing vitamin D by interacting with UV light. Its properties such as thickness and color can vary from subject to subject, and between different anatomical locations.[19, 25]

The skin consists of three primary layers, which can be further divided into finer layers consisting of specific types of cells. The three primary layers are, from top to bottom, epidermis, dermis and hypodermis.[19] A simplified model of the different layers of skin is shown in Fig. 1.

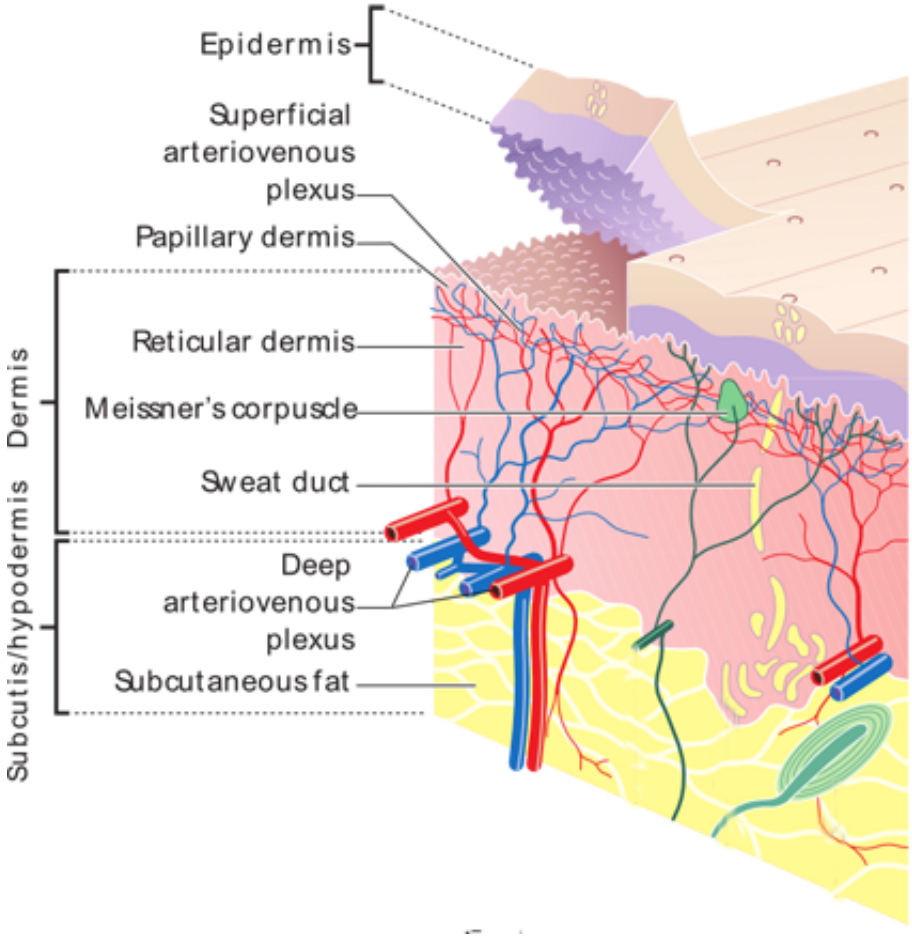

Figure 1: Structure of skin, showing the 3 layers, epidermis, dermis and hypodermis or subcutaneous tissue. Blood vessels are shown in red and blue. (Source: Wikimedia Commons, *http://commons.wikimedia.org*)

2.1.1 Epidermis

The epidermis is the thin surface layer of the skin, consisting mainly of keratinocyte cells that are shed off as new ones grow to replace them, renewing the surface structure constantly. These keratinocytes form a barrier protecting the body from most external effects[1, 20]. The overall thickness of the epidermal layer can vary from 0.05 to 1.5 mm, but is typically between 0.05 and 0.15 mm[21]. Considering its optical properties, the surface of the epidermis forms an optical boundary with air as its refractive index is commonly between 1.3 and 1.5[11]. Epidermis contains melanin, a pigment that affects the color of the skin, modifying the spectrum of reflected light[22].

The upper layer of the epidermis is the cornified layer, or stratum corneum, consisting of dead corneocyte cells. New keratinocyte cells that are produced in the lower layers propagate towards the surface as they undergo a process of cornification transforming them into non-living corneocytes. A constant shedding of the corneocytes from the surface of the skin maintains the thickness of this layer as new cells replace them. The thickness of the stratum corneum depends on the location, being thicker in areas that require additional protection such as soles and palms, but normally it contains 15 to 20 layers of cells.[19, 20, 21]

In areas of thick skin, a translucent layer, stratum lucidum, is located under the stratum corneum. It is very thin and does not have a clear boundary between the adjacent layers, consisting of flat keratinocytes. It can be neglected when the optical properties of skin are considered. Below the stratum corneum is the granular layer, or stratum granulosum, where the cells migrating to the surface of the skin become granular by creating lamellar bodies in the space between cells.[19, 21]

Below the stratum granulosum is the spinous layer, stratum spinosum, where the keratinocytes of the skin begin the keratinization process that will transfer them into corneocytes[22, 23]. New keratinocytes are constantly produced in the basal layer, or stratum basale, below this layer. The stratum basale also contains cells related with touch sensation, immunology and the production of melanin[22, 24].

2.1.2 Dermis

Beneath the epidermis lies the second primary layer of the skin, dermis. The dermis is connected to the epidermis by a basement membrane, and it acts as a cushion between the epidermis and the deeper body structures. It consists mostly of connective tissue, but it also has other structures such as glands and hair follicles. Also, whereas the epidermis is bloodless, the dermis contains capillaries and blood vessels[1]. Two clearly separate layers can be identified within the dermis, the papillary dermis and reticular dermis.[23, 26]

The papillary dermis, or stratum papillare, has cone-like extensions that attach it to the epidermal layer while at the same time maximizing the contact surface. These extensions are mainly constructed of areolar connective tissue, but they also contain blood capillaries that supply the dermis and epidermis with nutrition and transport waste.[23]

Below the stratum papillare lies the reticular layer, stratum reticulare, which consists of strong and elastic connective tissue.[27] The structure of the connective tissue is irregular with no clear pattern, which makes it difficult to create precise mathematical models of its behaviour. This structure enables the dermis to sustain strong forces. The weave-like structure is capable of bonding large amounts of water, which affects the absorption of light in the infrared range. The stratum reticular also contains more blood capillaries, larger blood vessels and receptors and glands.[23]

2.1.3 Hypodermis

The lowest layer of the skin, hypodermis or subcutaneous tissue, consists mainly of fat. It is attached to the deeper body structures by means of fibrous bands. Unlike the dermis and epidermis it does not have a layered structure, but consists of loosely connected tissue and fat lobules. It also contains blood vessels supplying the dermis, as well as hair follicle roots, nerve endings and even some small muscle structures.[23, 28]

2.2 Optical properties of skin

While the anatomical structure of skin and its different layers is well known, mathematical models of skin studying its optical properties often simplify this structure. Many models with varying degrees of complexity exist, and they

generally consist of a finite number of homogenous layers, each characterized by parameters such as coefficients for absorption and scattering[29, 30]. Adding the effect of pulsating blood into the models complicates them. For example, it is known that blood in vessels has an anisotropic nature due to the orientation of the red blood cells, and this anisotropy varies with the blood pulsations[31].

Considering the skin as an optical system, the behaviour of light in the three main layers varies greatly as they have very distinct structures. Firstly, the epidermis is bloodless tissue, and acts mainly as an absorbing medium with relatively low scattering and negligible temporal modulation over short time intervals[10]. Any pigmentation of the skin resides in the epidermis, and while different pigmentations can affect the overall transmitted light they cannot cause any modulation, keeping the signal to noise ratio of the modulated light versus total transmitted light constant[1, 10]. Because the epidermis is very thin, it's scattering and absorbing effects are small[10]. The underlying dermis contains blood capillaries in the papillary region which is in contact with the epidermis, and blood vessels in the lower reticular dermis. In this layer, the ratio of blood volume per tissue volume is typically between 0.05 and 0.15, depending on person, area of skin and external factors such as temperature[12].

For bloodless dermis, in vitro scattering and absorbing properties are known and it has been shown that the absorption coefficient is almost constant for wavelengths from 400 to 1000 nm, and the scattering coefficient decreases when moving towards the infrared wavelengths, which can be seen as an increased depth of penetration for infrared light[10, 11]. On the other hand, blood in the tissue as a mixture of venous and arterial blood has a constant scattering coefficient but its absorption coefficient depends on wavelength and also the concentration of oxygenated and deoxygenated haemoglobin in the blood[32]. The general behaviour of dermis can be approximated as a combination of the bloodless dermis and blood in tissue[10], but in reality the optical response of the system is very difficult to model accurately. The absorption coefficients of oxygenated and deoxygenated haemoglobin, melanin and bloodless skin in the visible and infrared region can be seen in Fig. 2.

With each cardiac cycle, the heart creates a pressure pulse that travels along the blood vessels. This pulse is smoothed as it travels, but it is still detectable even in the peripheral areas simply by pressing one's finger against the skin. The pressure pulse causes the blood vessels to expand and constrict

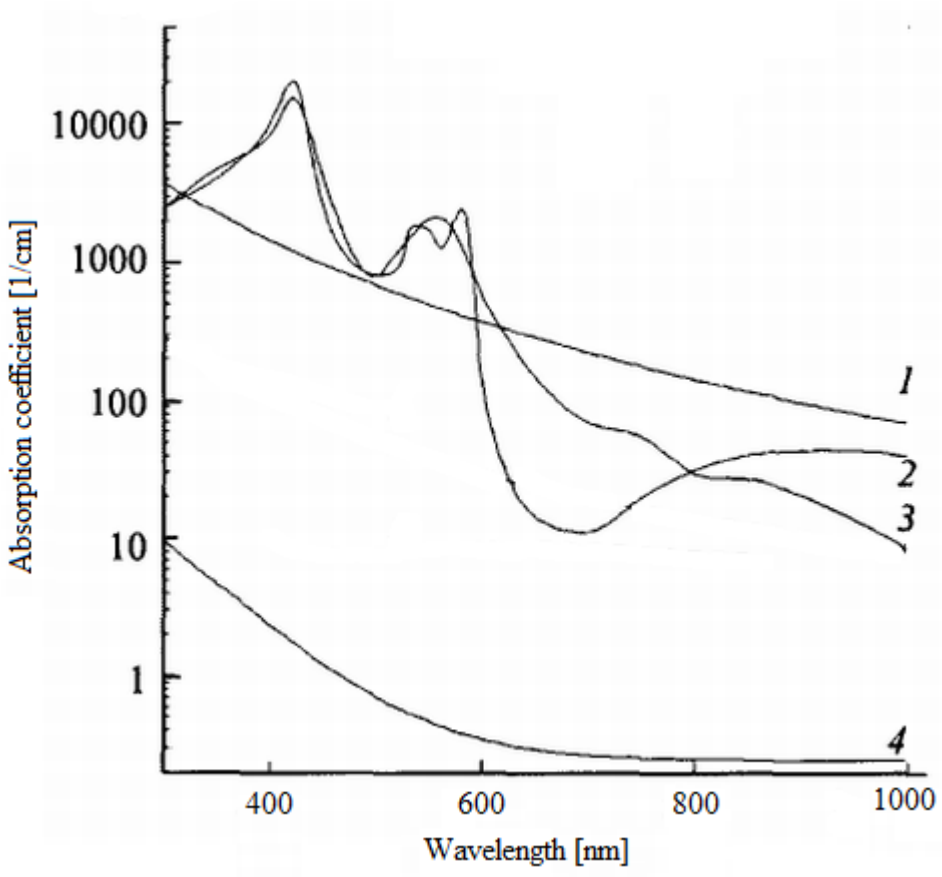

Figure 2: Absorption coefficients of melanin (1), oxygenated (2) and deoxygenated (3) haemoglobin and bloodless skin (4) as a function of wavelength of illumination[14]

and pushes the blood forward in the circulatory system. As the volume of the blood vessels changes, the relative amount of blood in an investigated area of skin also changes proportionally. This effect causes a modulation in the optical properties of skin, with the frequency of the heart beat. Breathing can also cause similar modulations but typically at lower frequencies.[33, 34]

The thickness of the dermis can range from 1 mm to 4 mm, but is typically under 2 mm[14, 50]. Approximate penetration depths for visible and near-infrared light are given in Table 1. From these values, it can be seen that the thickness of dermis is larger than the penetration depth of light. Wavelengths under 600 nm can reach the stratum papillare and the upper portion of stratum reticularis, which contains small capillaries. Longer wavelengths can penetrate deeper and reach the lower portion of the stratum reticularis which contains larger arteries and veins. Small amounts of light can penetrate through this layer and reach the hypodermis, which contains the body's subcutaneous fat storages[1, 10, 14].

Table 1: Approximate depth for penetration of optical radiation in fair Caucasian skin to a value of 1/e (37%) of the incident energy density[49]

Wavelength [nm]	Depth [μm]
400	90
450	150
500	230
600	550
700	750
800	1200
1000	1600

The small capillaries in the stratum papillare and upper portions of the reticular dermis form a horizontal blood net, the superficial arteriovenous plexus and the vessels in the lower dermis another layer, the deep arteriovenous plexus. These layers are also shown in Fig. 1. The blood vessels in the superficial plexus have a smaller diameter than those in the deeper plexus. Because of this, the relative blood volume in the lower levels of the dermis is higher[51]. This also affects the optical properties of skin, wavelengths of light with larger penetration depth can reach the deep arteriovenous plexus while shorter wavelengths are limited to the superficial plexus.

Although the structure of the hypodermis is different from the dermis, its optical behaviour is very similar compared with bloodless skin[13, 52]. As mentioned before, although the penetration depth is limited, small numbers of photons are still capable of penetrating deeper into the tissue. Hemodynamic imaging amplifies the signal in a way that makes it possible to receive information even from these photons, making it possible to gather data deeper from the skin.

The stratum reticulare contains large amounts of water, which also affects the optical properties of the skin. Fig. 3 shows the absorption coefficient of water for visible light. Water does not absorb visible light strongly, but the absorption coefficient increases when moving into infrared wavelengths.[53]

Considering the complex optical response of blood and the different layers of skin under different wavelengths and the method of signal generation for hemodynamic imaging, one can see that attempts to create an accurate prediction about the system's performance would be difficult and the accuracy

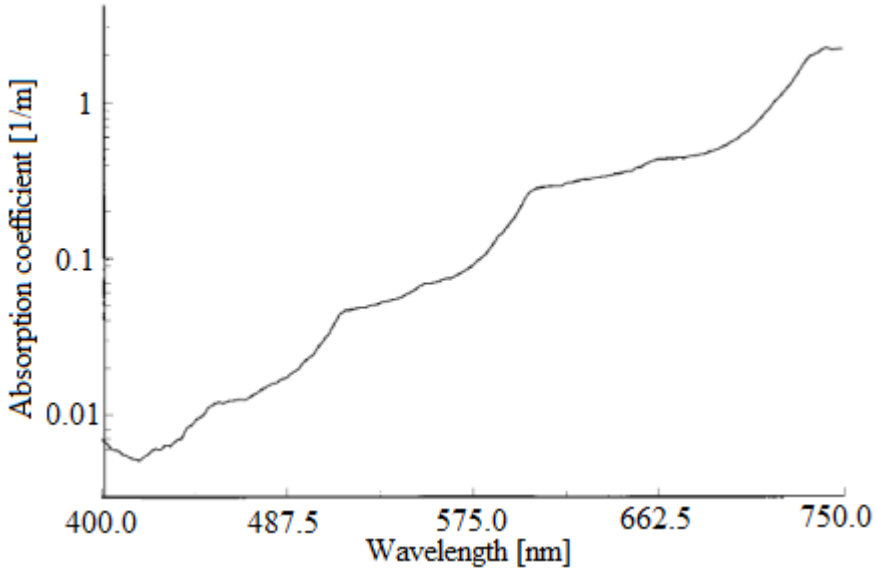

Figure 3: Absorption coefficient of water as a function of wavelength in the visible spectrum [53]

of the results could not be guaranteed. Therefore, the best way for studying this performance is by an experimental method using multiple repetitions and subjects to counter for the natural variations in skin.

3 Optical analysis methods

In this section we would like to present three optical techniques used for analyzing physical phenomenon related to the pulsations of blood, photoplethysmography (PPG), pulse oxymetry and laser Doppler flowmetry. In addition we will be presenting the principle of lock-in amplification, which is later applied to the method of hemodynamic imaging.

3.1 Photoplethysmography

The principle of PPG is closely connected to the process of hemodynamic imaging, as the first part of the data analysis is to produce a PPG graph showing light intensity variations in a chosen region of interest. PPG is an optical method measuring the volumetric change of the blood vessels caused by the heart beats, and it is used in hospitals to monitor the heart rate of patients and provide information about their condition.[5, 35]

As explained before, the pressure pulse caused by a cardiac cycle travels along the circulatory system causing volume changes in blood vessels, and the relative volume of blood in a given area changes. This change affects the optical properties of the tissue in a way that can be registered by the PPG device, producing a pulsating signal with the frequency of the heart beat.[5]

The PPG system consists of an illuminator and a detector. The illuminator can consist of one or more light sources, typically LEDs, which produce a steady illumination. The wavelength of the illumination can vary based on specific application, all wavelengths from green to near-infrared can produce a PPG signal. Most commonly used illuminators are green, red and near-infrared. Shorter wavelengths have smaller penetration depths making it impossible to obtain a signal from the pulsatile blood vessels. The detector is typically a photodiode, although devices which use a digital camera to gather information from a larger area are also available. Based on measurement geometry, the illuminator and detector can either be on the same side of the subject in reflection geometry or on opposite sides in transmission geometry.[5, 36]

As light from the illuminator enters the skin, it interacts with the tissue and blood. Some is scattered, and some is absorbed, and the overall intensity of light that is transmitted through the subject in transmission geometry or back-scattered away from it in reflection geometry is reduced. The optical

properties of blood are different from those of the surrounding tissue, so a change in the relative blood volume causes a change in the intensity of light at the detector after interaction with the tissue. The detector then converts the intensity variations into an electric signal, which can be visualized by an oscilloscope or used to calculate a numerical value for the heart rate. An example of a signal produced by the PPG compared with the signal of an electrocardiogram is shown in Fig. 4.[5, 35]

Figure 4: An example of a PPG signal and electrocardiogram (ECG) signal produced by heart beats[5]

A PPG system can be applied to a variety of different tasks. It is naturally capable of monitoring the heart rate, and also some properties of the cardiac cycle. It can be used to provide considerable underlying characteristics of blood circulation.[38] It is also possible to monitor respiration, as expansion and contraction of lungs during breathing causes a varying pressure on the heart in a process known as normal sinus arrhythmia. These changes of pressure affect the intracardial pressure, modulating the intensity of the pressure pulse caused by the heart beats. These low-frequency pressure variations can be detected by the PPG, as they affect the change in relative blood volume in tissue. The variations coincide with the breathing rate making it possible to determine inhaling and exhaling.[37]

As the PPG is directly monitoring the blood pulsations, it can also be used to detect conditions which alter the blood pulsation. One example is monitoring the level of anesthesia during surgery. A surgical incision can cause a response in the symphatetic nervous system increasing the intensity of the pressure pulse created by the heart, showing as an increased amplitude of the

PPG graph if the level of anesthesia is not sufficient[39]. Loss of blood due to extraction or severe bleeding can also be detected as they reduce the intravenous pressure thus lowering the amplitude of the PPG signal[40]. The technology can also be used together with other devices to provide more in-depth information about the health of patients or control some other processes, such as in pulse oxymetry and in hemodynamic imaging as demonstrated in this thesis.

Various commercial solutions for measuring the PPG can be found, with some variation in construction. Possibly the most popular design is a clip that attaches to the finger, with a light source on one side and a detector on the other, measuring the intensity of light that has travelled through the finger in transmission geometry. Other possible measurement locations are, for example, the earlobe, or even the genital area. Devices that operate in reflection geometry with the light source and detector being on the same side of the sample are less common and more varied in type, and can be used to measure a signal from various parts of the body by placing the device against an area of skin.

While the PPG system is useful in the field of medicine, it has drawbacks that reduce its usability in some situations. Main problems surrounding the use of a finger-type PPG device are the system's sensitivity for external interference and its inreliability in situations where blood flow in the extremities is weakened, such as during shock or hypothermia[42]. Slight movements of the device can disturb the signal, and external electric fields and light from the surroundings can modify it if the device is not shielded properly. The size of the sensors can also cause problems, if they are too large they will not have a steady contact with skin, and if they are too small they can cause a pressure on the skin weakening the blood flow. This is true also for sensors measuring the signal from other locations than the finger.[41]

A problem with all devices is the difficulty of quantitative analysis and comparison of results obtained from different patients and areas. Humans can have a large amount of variation in properties affecting the optical properties of skin, such as skin pigmentation and weak peripheral blood flow[6]. Due to these reasons it is difficult to use the PPG for anything besides observing the frequency of blood pulsations and detecting effects which can cause an abrupt change in their intensity.

The system of hemodynamic imaging captures images of an area of skin that is illuminated by a LED, and observes the average pixel intensity of the image frames in a chosen area over time to begin the data analysis. This method is effectively a non-contact PPG measurement, and the created signal resembles the PPG signal very closely. For hemodynamic imaging this step is creating a reference for the operation of the device.

3.2 Pulse oximetry

Another very well known optical technology whose operation is based on the pulsating nature of blood is the pulse oximetry. Like photoplethysmography, pulse oximetry also uses the changes in the intensity of light after it has travelled through skin with pulsating blood, but the method measures the ratio of oxygenated and deoxygenated haemoglobin in the blood. This value is also known as blood oxygen saturation. Fig. 5 shows an example of a commercial finger-attached pulse oximeter.[3]

Figure 5: A commercial finger-attached pulse oximeter, showing the oxygen saturation and heart rate. (Source: Wikimedia Commons, *http://commons.wikimedia.org*)

The main difference in the structure between a PPG sensor and a pulse oximeter is that while it is possible to have a PPG device with only one light source, a pulse oximeter always requires at least two light sources with different wavelengths. Typically one wavelength is 660 nm and the other between 900 and 940 nm. These light sources are turned on and off at a high fre-

quency so that only one is active at any time, which results in two separate signals resembling the PPG signal. The choice of these wavelengths is due to the absorption spectrum of oxygen saturated and unsaturated haemoglobin, as shown in Fig. 6.[3, 6]

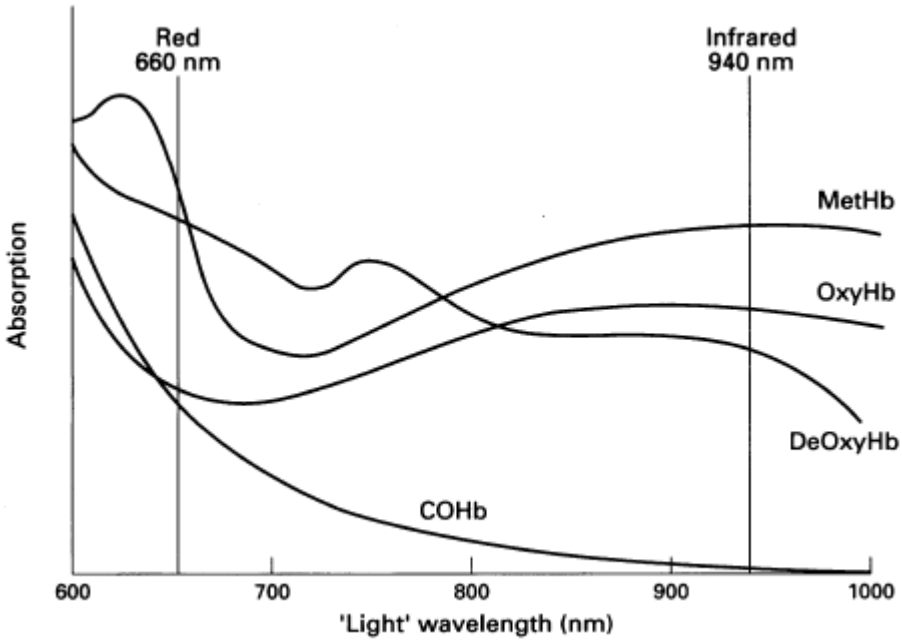

Figure 6: A graph showing the absorption of different types of haemoglobin at different wavelengths in arbitrary units. The absorption spectrum of oxygen saturated haemoglobin is marked with OxyHb, unsaturated with DeOxyHb, carboxyhaemoglobin with COHb and methaemoglobin with MetHb. Vertical lines mark the wavelengths 660 nm and 940 nm. [6]

Pulse oximetry assumes that any change in the light transmitted through the measured object over short time intervals is caused to the pulsations of blood. Therefore, knowing the original intensity of light we can separate the absorption of light caused by the surrounding tissue from the absorption caused by the presence of pulsating blood by separating the nonchanging DC component of the signal from the pulsating AC component. Neglecting the DC component, we obtain two slightly different varying signals, one for each wavelength.[3]

As can be seen from Fig. 4, the rate of absorption for oxygen saturated haemoglobin at 660 nm is lower than for unsaturated, whereas at 940 nm the absorption coefficient of oxygenated haemoglobin is slightly higher. Therefore, if we calculate the absorption of light caused by the presence of saturated and unsaturated haemoglobin from signals obtained at with the two used wave-

lengths and compare their ratio, we can obtain a value that corresponds to a specific value of blood oxygen saturation, notated by SpO_2. Instead of calculating the result, many devices use a look-up table with pre-calculated values to find the solution.[3]

The principle of pulse oximetry is very similar to the idea of photoplethysmography, so it also suffers from the same limitations with it: movements of the detector cause changes in the signal, external light can distort it and weakened blood flow can make it impossible to acquire any signal. Pulse oximetry also has some limitations due to its method of operation and the physical and physiological properties related to its signal formation. For example, the presence of carbon monoxide saturated haemoglobin during carbon monoxide poisoning can lead to erroneous measurement results[44], and an increased concentration of methaemoglobin which cannot bind oxygen will cause a pulse oximeter to show a reading of 85% regardless of situation[43].

There are also problems with pulse oximetry related to misconceptions about its capabilities. Although it is a useful tool in monitoring the condition of patients, it only provides information about the content of oxygenated haemoglobin in pulsating arterial blood, and does not give a complete picture of the metabolism of oxygen in the body, other methods such as blood gas analysis and monitoring of exhaled CO_2 should also be used in conjunction with it[6]. Pulse oximetry is still a very essential and powerful tool for detecting problems with oxygen saturation, which is very critical during surgical operations, intensive care and emergency situations. Lack of oxygen can cause severe brain damage in a matter of minutes and detecting it as soon as possible will greatly improve the survivability of patients.

3.3 Laser Doppler flowmetry

Laser Doppler flowmeter is a noninvasive method for measuring the velocity of red blood cells propagating with the microcirculatory blood flow in the dermis. It uses a laser light source and a photodetector, measuring the Doppler shift of the light as it is scattered from the moving blood cells. It can be used to study the blood circulation reliably and with good sensitivity.[54, 55]

Laser light is monochromatic, ideally containing only light of one wavelength. When this light enters the tissue, it scatters multiple times either

from stationary or moving structures. Scattering from stationary subjects such as the connective tissue of the dermis does not change the properties of the light, but moving structures such as blood cells cause a Doppler shift in the wavelength of light scattered from them.[54, 55]

After light has scattered multiple times inside the tissue the direction in which it is moving is completely random, meaning that when it interacts with blood flowing in a constant direction the Doppler shift can either increase or decrease its wavelength. This can be seen as a broadening of the spectrum of the laser light that is back-scattered from the tissue. The change of the spectrum is directly related to the velocity of the scattering particles.[54, 55]

As the light with a broadened spectrum arrives to the photodetector, it interacts with light that was back-scattered only by stationary structures and has maintained its wavelength. After superposition, the different waveforms produce a beating effect, causing a fluctuation in the observed light intensity. By studying this fluctuation, it is possible to calculate the shift in wavelength caused by the Doppler effect and thus the velocity of the scattering blood cells.[54, 55]

A laser Doppler flowmeter can be used to measure the speed of the blood flow in one point or a larger area. The laser beam can be widened and the back-scattered light collected to a camera using focusing optics. Using the same principle as before, the method can produce a 2D image of the speed of blood flow in a section of the skin. This way, it can be used to detect regional anomalities in blood flow.[56]

3.4 Lock-in amplification

Lock-in amplification is a signal processing method for amplifying the signal-to-noise ratio of sinusoid signals in certain situations. It is not limited to optical systems and is not considered an "optical method", but in this thesis we will discuss it briefly because hemodynamic imaging uses a slightly modified version of it in its data analysis process.

Lock-in amplification can be used to recover a signal in situations where the signal-to-noise ratio is very low, even much smaller than 1[46]. It requires that the carrier wave of the signal is known and can be used as a reference

for the recovery of the signal. The method is also phase sensitive, so it can be used to detect the phase shift of pulsating signals in relation to the known carrier wave. If the carrier wave of a signal is not known, lock-in amplification is not applicable.[45]

The operation of lock-in amplifiers is based on the mathematic principle, that when a sinusoid function with a frequency f is multiplied by another sinusoid with a different frequency or phase and integrated over time, the result is zero. This is called orthogonality of sinusoid functions. If the frequency and the phase of the multiplying signal are the same with the original, the integral gives a nonzero value related to the amplitudes of the two signals.[47, 48]

During its operation, a lock-in amplifier multiplies the values of the observed signal with a second signal derived from the carrier wave of the signal. This second signal is called the reference signal, or reference function. The result is then integrated over a time period much longer than the period of the signal. Any component of the investigated signal that has a different frequency or phase compared to the reference signal is reduced to zero. This process yields a value for the amplitude of the reference signal, and repeating it for the length of the entire signal duration we can observe the amplitude and its variations very clearly.[47, 48]

Lock-in amplification can extract the signal from the noise because in many cases, noise has a much wider frequency spectrum. Therefore, even if the effects of noise completely cover the signal when observed temporally, in a specific frequency spectrum the amplitude of signal can be larger than the amplitude of noise. However, if some source produces noise specifically with the same frequency as the signal, even lock-in amplification cannot help in removing its effects.[15, 47, 48]

A simple example of the performance of lock-in amplification is shown in Fig. 7. The figure shows how the change of a signal's amplitude can be detected even from very noisy signal. The image was created using a simple algorithm for lock-in amplification, calculating the definite integral of the product between the noisy signal and sinusoid reference signal with constant amplitude along different intervals of the signal. More advanced methods can produce better results.[47, 48]

A modified version of lock-in amplification is used in hemodynamic imaging

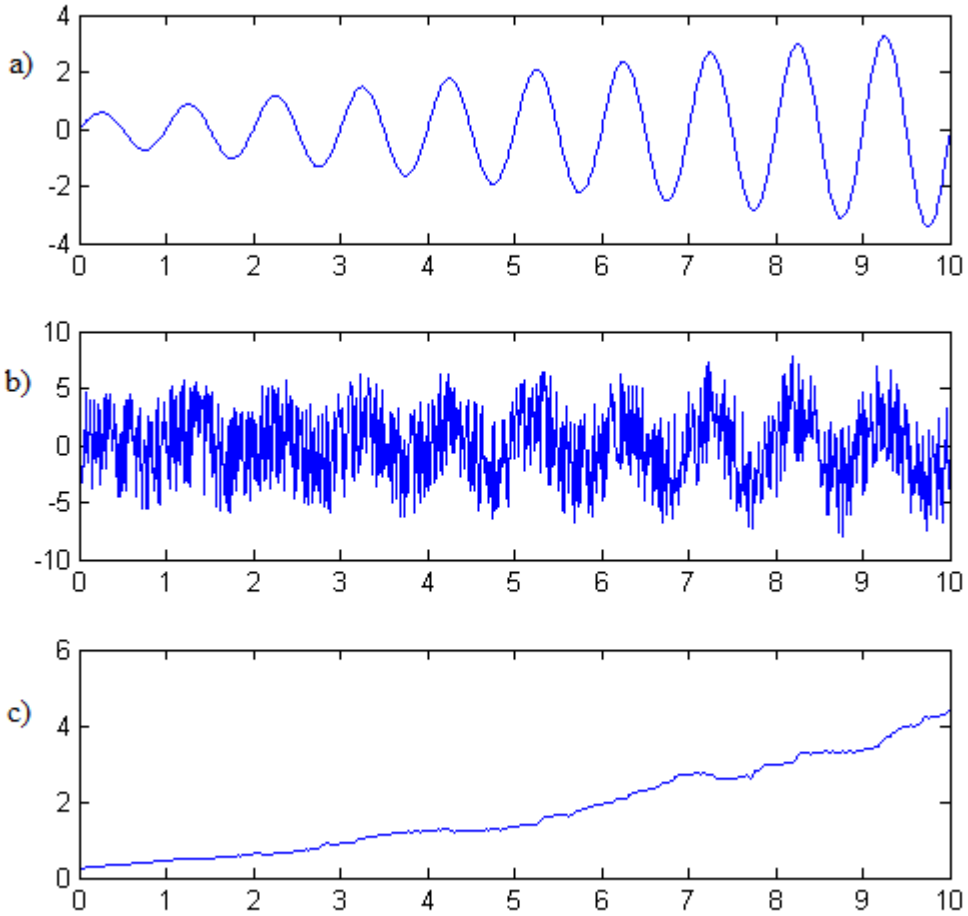

Figure 7: A figure showing the performance of simple lock-in amplification created with MATLAB; a) shows a sinusoidal signal with a steadily increasing amplitude, b) the same signal after addition of high-amplitude noise and c) the result of lock-in amplification, clearly showing the rising trend in amplitude. The steepness of the curve in the third image is not to scale.

to detect the amplitude of blood pulsations related to the process of heart beat. The method is applied to pixel values of images captured from a target, extracting the amplitude of pulsations from signal with very low signal-to-noise ratio.

4 Method of operation

4.1 General structure of device

The measurement system used for hemodynamic imaging is simple, consisting of three main parts: illuminator, camera and computer. This simplicity makes hemodynamic imaging attractive for clinical use, as the system is affordable and easy to move and operate without special training.[9]

The illuminator of the system can be any kind of constant light source that is powerful enough to illuminate the observed area evenly. Previous experiments have shown that regular high-power LEDs can be used to reliably operate the system. The illumination must be constant, meaning that the intensity and wavelength will not vary during the course of measurements. Illuminators powered by AC voltage cannot be used, as their behaviour changes with the frequency of the modulation of the voltage. The issue of the optimal wavelength of illumination is discussed later.[9]

The illuminator is coupled with a linear polarizer, which will cause the light to be polarized. This will cause a drop in the overall intensity of light, which should be taken into consideration when choosing a light source. Other elements, such as focusing mirrors or lenses to modify the path of light, or diffusors to make the distribution of light smoother can also be used to improve the illuminator. For example, the intensity distribution of the light of some LEDs correlates with the structure of the active zone in the LED, causing an image of the active zone to be formed on a shader placed in front of it. This can be countered by using a diffusor.[9]

The second part of the system is a digital camera capable of capturing monochrome images continuously at a high frame rate in a non-compressed format such as bitmap images. The required resolution of the camera depends on quality of measurements and the size of the measured object and its distance from the camera. Focusing optics are required to form an image on the camera's sensor, commercially available camera objectives can be used for this purpose. Image acquisition is similar to normal photography and therefore it is not necessary to build customized camera optics. The camera should be placed at an angle normal to the measured object's surface to maximize the signal-to-noise ratio, and the illuminator should be close to this angle and the path of light free from obstacles.[9]

The camera and its objective also require a linear polarizer, whose axis of polarization is perpendicular to the polarizer coupled with the illuminator. Light which reflects from the surface of the skin contains no information about the pulsation of blood inside the tissue, and it is filtered out using the polarizers. As the polarized light from the illuminator reflects from the surface of the palm, it maintains its polarization state and is filtered by the second polarizer whose polarization axis is perpendicular to this state. Light which is transmitted inside the tissue changes its polarization state before it is backscattered and detected by the camera, so the second polarizer has a smaller effect on its intensity.[9]

The final component of the measurement system is the computer, which is controlling the operation of the camera and recording the captured images. It is possible to analyze the captured images as they are being recorded and conduct the measurements in real time, but this requires more advanced software and more processing power. If the images are analyzed after the measurement is complete, any modern low-end laptop computer is sufficient to operate the system. The main limitations are storage space and memory, if we capture uncompressed bitmap images at 10 frames per second for 5 minutes we receive 3000 images. If the image resolution is 640 by 480 pixels and the image bit depth is 8 bits, the size of one image is 300 kilobytes and the total size for all images approximately 890 megabytes.[9]

These are the necessary components of the measurement system, but it is possible to refine the system by adding other parts. For example, external light can reduce the quality of the results but adding a protective screen can block out this light, and a support or frame can prevent involuntary movements of the subject during measurements. These kinds of additions are not necessary for the basic operation of the system, but they can improve its performance under some circumstances. A crude presentation of the device can be seen in Fig. 8.[9]

4.2 Structure of our device

The hemodynamic imaging system developed by our research group follows the general form presented in the previous chapter, but improvements have been made to it. The hardware and software of the system have been optimized for ongoing clinical experiments to improve the reliability and smoothness of operation.

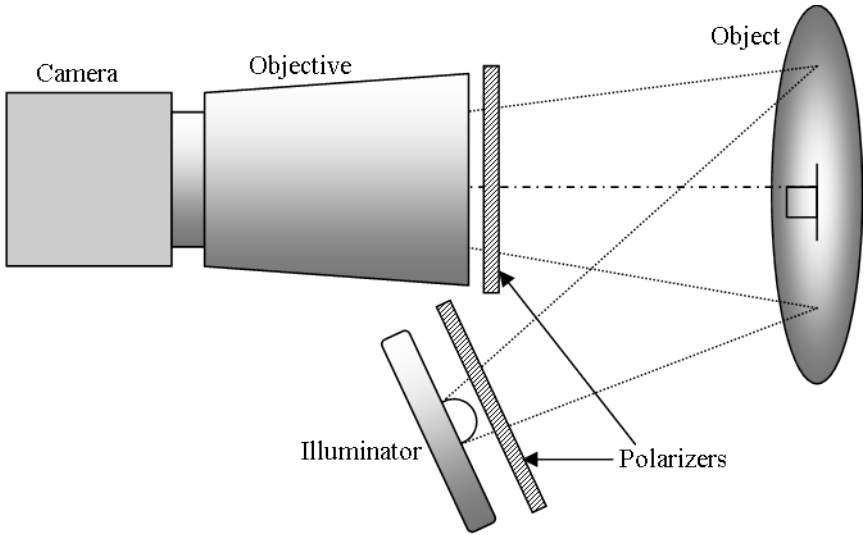

Figure 8: Crude presentation of the hemodynamic imaging system, showing the illuminator, object, camera with objective and polarizers

The illuminator of the system can house up to four high-power hexagonal LEDs which can be interchanged freely. The LEDs currently in use are Hexagonal Package High Power Single Chip LEDs by Roithner Lasertechnik GMBH, with wavelengths available from 460 to 920 nm. The LEDs can be activated in sets of two to achieve high-power illumination, for example a total of 110 lm with 520 nm LEDs. The polarizer is made from gray visible linear polarizing film by Edmund Optics, which functions well in the visible light area. The illuminator is cooled by a small fan and heat sink to guarantee steady operation over long periods of time.

The currently used camera is EO-1312M 1/2C̈MOS Monochrome USB Camera by Edmund Optics, which is connected to the computer via a USB2.0 connection. The camera's maximum resolution is 1280x1024 and it is capable of capturing images at 25 frames per second. The camera is used with Canon TV Zoom Lens V6x18, 18-108 mm, 1:1.6 camera objective. A polarizer which is made from the same polarizing film as for the illuminator is fixed in front of the objective so that its polarization axis can be adjusted freely. The illuminator of the system is mounted together with the camera, and the combination is supported by a regular photography tripod.

The computer operating the image acquisition is Fujitsu Siemens Lifebook S6410 with Intel Core2 Duo processor and 2GB of RAM. The software for controlling the camera was custom made based on a Microsoft Visual Studio C++ software development kit supplied by the camera manufacturer. The

program can control the camera's properties, such as pixel clock, frame rate, exposure time, image size and the amount of pictures captured. It has a preview mode which allows the user to inspect and adjust the image properties and histogram before starting, and it can record images as single separate frames or groups of several frames. The image analysis is conducted with the same computer using MathWorks MATLAB, the analysis method is discussed later. Fig. 9 shows the current version of the system.

Figure 9: The current version of the hemodynamic imaging system, showing the camera and objective with attached illuminator supported on a tripod.

4.3 Description of measurement

The measurement device and measurement protocol are simple, and the measurements can be conducted with minimal training. The main task is to position the camera and the illuminator so, that the observed skin area is completely visible ad facing the camera directly, and the illumination intensity is not too high to cause saturation of the images. Our group has developed standard procedures for different types of measurements, such as measuring the skin on the palm or the face, but these are modifiable to satisfy different conditions.[9]

It is important to eliminate external illumination, especially if it is not uniform spatially and more importantly, temporally. Normal lamps powered by AC current are constantly blinking at a frequency that the human eye

cannot discern, but this blinking is clearly visible in the high-speed images taken during the measurements. It is also important to eliminate involuntary movement, there are some computational algorithms to remove the effects of movement from the measurements but it is better if this movement can be reduced. Completely fixing the subject to an immovable frame is not good as it can hinder the blood circulation and therefore affect the signal, supports which allow the studied area to be relaxed and without tension are preferred.[9]

After the subject is prepared, the camera and illuminator are placed. The camera should be close so that the entire observed area is visible in the image and the camera is facing the surface of the skin directly. The illuminator should be placed so that it can provide an optimally uniform illumination on the observed area, without being in the camera's line of sight. After both have been placed, the polarizers of the system should be adjusted so that their polarization axises are perpendicular to each other. This can be done by placing a reflecting object, such as a small mirror, in the camera's field of view and observing its brightness as one of the polarizers is rotated. When the brightness reaches a minimum, the polarization axises are correct. The reflecting object should appear almost completely dark.[9]

After the mechanical setup is complete, the level of observed intensity at the camera is adjusted, by changing either the intensity of illumination or the exposure time of the camera. A histogram showing the pixel intensity distribution can be used to enable easy adjustments. For example, darker skin pigmentation will cause an overall drop in reflected light intensity which is hard to predict precisely without a histogram to aid in the process. The illumination should be adjusted so that the maximum image intensity is close to the maximum of the dynamic range of the camera, in previous experiments keeping the maximum peak of the histogram at approximately 75% of the maximum intensity has been found best.[9]

Once the setup is ready, the measurements can be initiated. Processes after this can be automated. Once the images are captured the data analysis can operate with or without user input, as desired. The results can be shown immediately or kept for further study which supports both clinical and scientific use of the device.

4.4 Data analysis

While the operation of the measurement device is simple, the data analysis makes it different from other devices operating under the same principles. The analysis is based on the idea, that while pressure waves related with cardiac cycles travel along the blood circulation system, they cause a periodical modulation of local blood volume in the arteries and veins which affects the total intensity of back-scattered light after multiple scatterings. The modulations follow the same frequency with the heart beat. This section aims to explain the process of creating an image of the dynamic nature of blood using an example.[9]

To explain the data analysis, let us assume that we have captured 100 image frames from an arbitrary sample, with a frame rate of 10 frames per second. Let us assume that the image size is 640x480 pixels, and the bit depth is 8 bits. We can consider each image as a matrix A_m, where $\{m \in \mathbb{N} | 1 \leq m \leq 100\}$ is the index of the image in the sequence. Each matrix consists of elements a_{ij}, where $\{i, j \in \mathbb{N} | 1 \leq i \leq 480, 1 \leq i \leq 640\}$. Also, for each element $\{a_{ij} \in \mathbb{N}_0 | 0 \leq a_{ij}\}$. As the bit depth of the camera is 8 bits, the initial maximum value for each element is 255, but during the course of analysis this maximum can be exceeded.

To begin the analysis, we first consider one imperfection of the imaging system: the response of the camera is not perfectly linearly dependent on the intensity of adjacent light on the camera's sensor. It is therefore necessary to adjust the intensity values by multiplying them with experimentally acquired correction factors b_n, where $\{n \in \mathbb{N}_0 | 0 \leq n \leq 255\}$ is the index corresponding for each pixel value. However, to facilitate the process we can approximate the camera response to be linear at lower intensities, and nonlinear only when pixel values exceed 150. In this case, we can calculate from each matrix A_m a new corrected matrix A'_m, whose elements are

$$a'_{ij} = a_{ij} b_k, \tag{1}$$

where $b_k = b_{a_{ij}}$ when $a_{ij} > 150$, and otherwise $b_k = 1$. From previous experiments, we have calculated values for b_k to be approximately between 1 and 1.3.

We then begin to form an average pixel intensity graph, by calculating the average value of the elements in some predefined area of each matrix. It is not necessary to always calculate the average value of all the elements in each matrix, for example if there is a specific area of interest, or if the image area

is large. For this example, let us calculate the average from a 320x240 area in the center of the matrix in the following fashion

$$\hat{A}'_m = \frac{\sum_{j=160}^{480} \sum_{i=120}^{360} A'_m}{320 \cdot 240}. \tag{2}$$

If we now consider these average values to be the discrete values of a time dependent function $f_k(t_m)$, so that

$$f_k(t_m) = \hat{A}'_m, m = 1, 2, ..., 100 \tag{3}$$

we can consider the data as variation of intensity over time.

From this data we can already see pulsations with a regular frequency related to the heart beats, but the signal is obstructed by low-frequency variations due to breathing and movement, and it also has some high-frequency noise. Therefore, to make automatic detection of the correct signal frequency easier, we filter the signal first two times with a high-pass filter and then once with a low-pass filter, which results in removal of low-frequency variations and trends, and the removal of noise. The signal itself also becomes slightly rounded, but still maintains its visibility and is easier to detect. Let us mark this filtered signal as $\hat{f}_k(t_m)$.

To estimate the frequency of the pulsation signal we calculate its discrete Fourier transform and power spectrum. The formula for discrete Fourier transform is

$$F_k(\nu) = \sum_{t_m=1}^{100} \hat{f}_k(t_m) \omega_N^{(t_m-1)(\nu-1)}, \tag{4}$$

where $\omega_N = e^{(-2\pi i)/100}$, and the power spectrum is calculated as the modulus of the Fourier transform,

$$\hat{F}_k(\nu) = |F_k(\nu)|^2. \tag{5}$$

From this, we can see the frequency distribution of the signal, with typically a clear peak visible in the vicinity of 1 Hz, which corresponds to the heart rate 60 bpm. By setting limits for the expected value of the frequency it's possible to detect it automatically, ignoring the high-intensity low-frequency peaks which are typically present.

Once we know the frequency of the heart beat, we can start to enhance our signal by using a modified version of lock-in amplification. By comparing the measured signal with a reference frequency, it can greatly improve the signal-

to-noise ratio. Lock-in amplification is phase sensitive, which makes it well suited to our situation, where we can detect the frequency of the modulations caused by the blood pulsations from the average pixel values over time. By applying the method of lock-in amplification to the elements of the matrices representing pixels in the image, we can enhance the intensity variations with the correct frequency in those pixels. To begin the lock-in amplification we must first create a reference function which is then used for synchronous amplification of each pixel in the sequence of image frames.[9, 45]

The reference function for each measurement is created by choosing a narrow frequency band around the detected heart beat frequency, and then truncating the Fourier transform so that only the values in the chosen band remain while others are set to zero. To create the reference function we then apply the discrete inverse Fourier transform, which is of the form

$$R(t_m) = \frac{1}{100} \sum_{\nu=1}^{100} F_t(\nu) \omega_N^{-(t_m-1)(\nu-1)}, \tag{6}$$

where $R(t_m)$ is the discrete valued reference function, and $F_t(\nu)$ the truncated Fourier transform of the average intensity signal. As can be seen, the reference function is complex valued, and further analysis will show that its real part is in phase with the average intensity signal, and the real and imaginary parts are orthogonal to each other. As the reference function is created based on frames captured by the camera the system is self-referenced, requiring no outside input.

The frequency of heart beats and therefore the intensity modulations of back-scattered light are not always regular over the course of the measurement, even over short periods of time. Therefore, before the reference function can be used we must adjust it so that each maximum coincides with a respective maximum in the average intensity variations. This can be achieved by an adaptive algorithm that checks the maxima and adjusts them accordingly. After this, the reference function must be normalized so that the results calculated using it are comparable with other measurements. The normalization is done so, that

$$\sum_{t_m} Re[\hat{R}(t_m)] \hat{R}(t_m) = 1, \tag{7}$$

where $\hat{R}(t_m)$ is the normalized reference function. After the normalization, each image matrix A_m is multiplied with a corresponding value of the reference function, so that each element of the first matrix is multiplied with the first

value of the reference function, the second matrix with the second value and so on. The resulting complex-valued matrices are then summarized to form the correlation matrix, so that

$$S_c = \sum_{t_m} a_{ij}(t_m)\hat{R}(t_m), \tag{8}$$

where S_c is the correlation matrix. To complete the analysis, the correlation matrix is normalized by dividing each element with number of matrices used to create it, therefore forming an average correlation matrix, and finally by dividing each value of the matrix with a value from the corresponding location from a time-averaged image matrix. We notate this normalized correlation matrix with $\hat{S}_c$.[9]

The correlation matrix is the result of lock-in amplification on the pixel values varying in time synchronously with the heart beats. It is complex valued, and the modulus of each pixel value of the matrix is proportional to the amplitude modulation of the pixels, and therefore the amplitude of modulation of light reflected from skin. As this modulation is caused by the blood pulsations related with the heart beat, the correlation matrix describes the spatial distribution of the blood volume pulsations at the heart beat frequency. It is possible to form an animation describing the propagation of a "pulse wave", or relative phase of the complex blood pulsations in respect to the reference function in the skin by comparing the phase angle of the matrix in different locations.[9]

The analysis method described in this chapter is functional, but it contains many simplifications and omits details. Its main purpose is to explain the principles of the process. Also, real measurements are longer than the 100 frames used in this example, but the same method of analysis is simply used over multiple cycles to go through all the frames of the measurement, resulting in several correlation matrices which can then be analyzed together or separately. It is possible to begin analyzing the measurement data even before all measurements are complete, and the analysis is compatible with paraller processing making it possible to reduce the time of measurements and analysis. Even real-time measurements can be considered if the processing speed can be optimized.

5 Measurements, materials and methods

In previous chapters it was mentioned that the absorption coefficient of blood varies based on wavelength of illumination and blood oxygenation. The complex behaviour of skin and blood pulsations make it difficult to create an accurate model for the signal formation process of hemodynamic imaging. In any case the behaviour of the system will vary based on the used wavelength. Wavelengths under 600 nm are strongly absorbed by blood[14], and moving into deeper infrared (800 - 900 nm) the predicted penetration depth increases[49], making it possible to detect blood pulsations originating from deeper skin layers.

Based on this, we conducted a series of measurements to compare the blood pulsation signal amplitudes measured using different wavelengths of illumination. We chose 7 different wavelengths across the visible and near infrared spectrum with some consideration into theoretical values for absorption of light for oxygenated and deoxygenated blood, and availability of high-intensity light emitting diodes. The chosen wavelengths were 460, 498, 521, 623, 728, 811 and 920 nm. The measurements were conducted by using two volunteers, so that each wavelength was measured separately for both subject. The area of measurement was chosen to be the right palm, based on the high concentration of capillaries in the area[10].

For the measurements, the subjects were in sitting position with the palm of the right hand placed on an adjustable support at heart level, supporting the fingers and minimizing involuntaryy movement. The camera was placed facing the palm directly, so that the distance between the palm and the front lens of the camera objective was approximately 75 cm. The illuminator was attached to a rail that allowed it to be moved linearly towards and away from the palm, at an angle of approximately 10 degrees from the normal of the palm. The distance of the illuminator was adjusted to achieve optimal illumination with each LED. To polarize and filter the surface-reflected light from the measurements, polarizing film was used for the LEDs in visible spectrum and separate polarizers for LEDs in the infrared range, as the performance of the polarizing film decreases with wavelengths longer than 700 nm. One polarizer was placed in front of the LED and another was attached to the front of the objective so that it could be adjusted to find the correct axis of polarization. In addition, a small parabolic mirror with a piece of semitransparent tape was attached to each LED to collect the light and make it more diffuse to create an optimal

illumination spot. The measurement setup can be seen in Fig. 10.

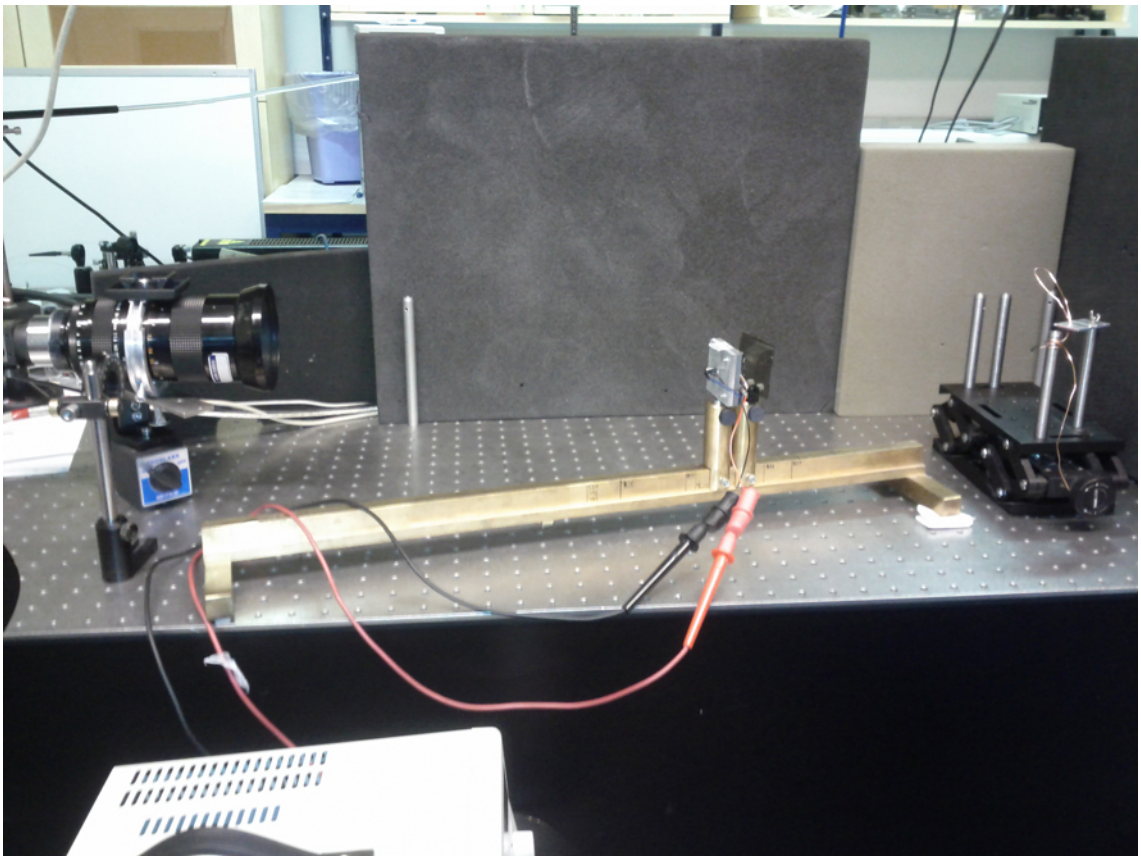

Figure 10: Measurement setup. On the left side, the camera and objective, in the middle the illuminator attached to a rail, and on right side adjustable support for the palm. During the measurements the lights in the room are turned off, and the surrounding shaders block off other external light.

Image capture was conducted at 10.69 frames per second, with image size 640x480 pixels. The images were saved as uncompressed 8-bit bitmap images. For each measurement, 600 frames were captured, making the total duration of one measurement approximately 56 seconds. For each measurement, after placing the LED and the parabolic mirror, the distance of the LED from the palm and the current of the LED were adjusted while monitoring the histogram of the image frames so that the peak pixel intensity was approximately 75% of the maximum pixel intensity to avoid saturation. After one measurement was complete, a new LED was changed and the adjustments were repeated before new measurements. For LEDs in the infrared spectrum the polarizers were changed to ones more suitable for infrared light, and the focus of the camera objective was adjusted, as infrared light behaves differently from visible light in regular camera objectives.

Once the measurements were complete, the results were analyzed by using a windowing algorithm, which takes 100 consequent measured frames and applies the method of lock-in amplification described before, resulting in a correlation matrix for those frames, and then moves forward by 20 frames and chooses another 100 consequent frames for the next analysis. Using this method we can choose a total of 50 slightly different subsets of the captured frames, therefore acquiring 50 correlation matrices. While there is some overlap in the image frames used for each analysis, each correlation matrix is unique due to the nature of the analysis.

An average pulsation amplitude image was formed by calculating the average of the complex modulus for each 50 correlation matrices, thus resulting in 7 pulsation amplitude images for both subjects, where each image represents the average pulsation amplitude observed at one wavelength. From these average images, an area with size of 150x120 pixels was chosen so that in each image an amplitude maximum could be observed within the area. Using this area as a limit, an average of the pulsation amplitude was then calculated within it from the complex modulus of each correlation matrix, thus resulting in 50 pulsation amplitude values for each wavelength. The final result is the average of these values, giving us a single, comparable value for the pulsation amplitude for each each wavelength in arbitrary units.

6 Results and discussion

After the correlation matrices were created, an average pulsation amplitude image was calculated using the complex modulus of each matrix. An example of such image is shown in Fig 11. Using these figures, an area with size 150x120 pixels was chosen so that with each wavelength a peak in amplitude values occurred within the area. Average amplitude values were then calculated within this area. The results obtained for both subjects are shown in Fig 12. The red lines show the pulsation amplitude at each wavelengths for 50 separate repetitions, and the blue line shows the average of these repetitions.

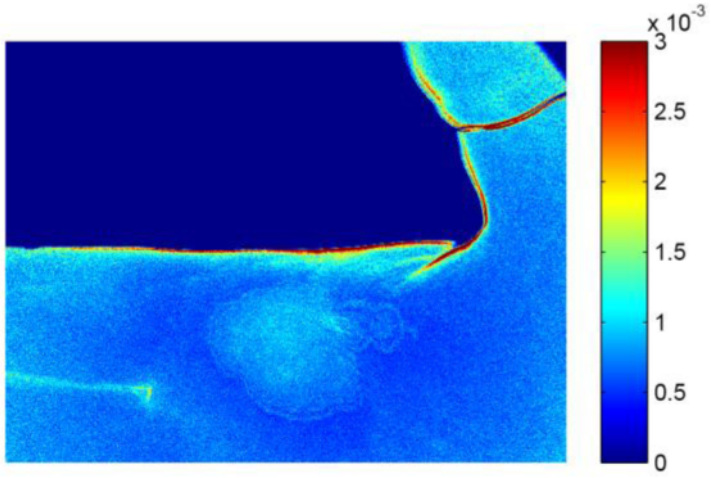

Figure 11: An example image showing the average pulsation amplitude distribution in the studied area.

Measurements from both subjects show the same behaviour, a local maximum in pulsations amplitudes was obtained using LEDs at 521 nm and 811 nm, and a minimum was observed at 623 nm. However it can be seen that each measured wavelength did produce a signal, and the differences between wavelengths in these measurements are not very large. Comparing the measurement scheme and previously recorded information about the behaviour of light in skin it can be assumed that there are no abrupt changes in amplitude between the measured wavelengths.

The appearance of a peak at 521 was expected, as the wavelength is absorbed strongly by both oxygenated and deoxygenated haemoglobin and its penetration depth is large enough to reach the superficial arteriovenous plexus that has a high concentration of capillaries. Shorter wavelengths are also absorbed strongly but their penetration depths are too small to be fully effective.[14, 49]

The decrease in amplitude and presence of a minimum at 623 nm corresponds with the abrupt decrease in the absorption coefficients of haemoglobin, and is likely caused by it. Reduced absorption means less interaction between the light and the pulsating blood, resulting in weaker signal. The penetration depth of this wavelength is not yet large enough to reach the deep arteriovenous plexus where the concentration of blood is relatively higher due to the presence of larger blood vessels.[14, 49]

Moving towards 811 nm we can see an increase in the measured amplitude of pulsations, which is most likely caused by the increase in penetration depth. The absorption coefficient of oxygenated haemoglobin also also increases slightly in this area, and as the penetration depth increases we can obtain a stronger pulsation signal from the deep arteriovenous plexus. The absorption coefficient of water also increases when moving towards the infrared wavelengths, which causes a decrease in amplitude as the water in tissue is not pulsatile.[14, 49, 53]

The local maximum at 811 nm is close to the small local maximum in the absorption coefficient of oxygenated haemoglobin. Also, the penetration depth at this wavelength should be large enough to reach the larger blood vessels in the lower area of the dermis. The decrease in amplitude after this maximum is most likely caused by two factors: the camera's decreased performance at infrared wavelengths and the rapidly increasing absorption coefficient of water. The penetration depth at these wavelengths is high enough to reach the hypodermis, but as it consists mainly of fat it does not improve the signal amplitude.[14, 49]

It can be seen that the amplitude of the pulsations has a very strong correlation with the absorption coefficients of haemoglobin, especially oxygenated haemoglobin. The locations of minima and maxima coincide very clearly. Based on this using illumination with wavelength just below 600 nm could produce a stronger signal, as a maximum of the absorption coefficient is located at that range. Also, using a camera that is more sensitive for the infrared wavelengths it could be possible to see an increase in the signal amplitude at the near-infrared spectrum.

Based on these measurements, other possible improvements for the system could be related with the software. As can be seen in Fig. 12, there are still

some artifacts in the results that differ from the average value at some wavelengths. Two most likely causes for them are movements of the subject and unsuccesful detection of heart rate. An algorithm for movement-related corrections has already been developed but still requires testing, and any changes which improve the quality of the signal also improve the detection of the heart rate.

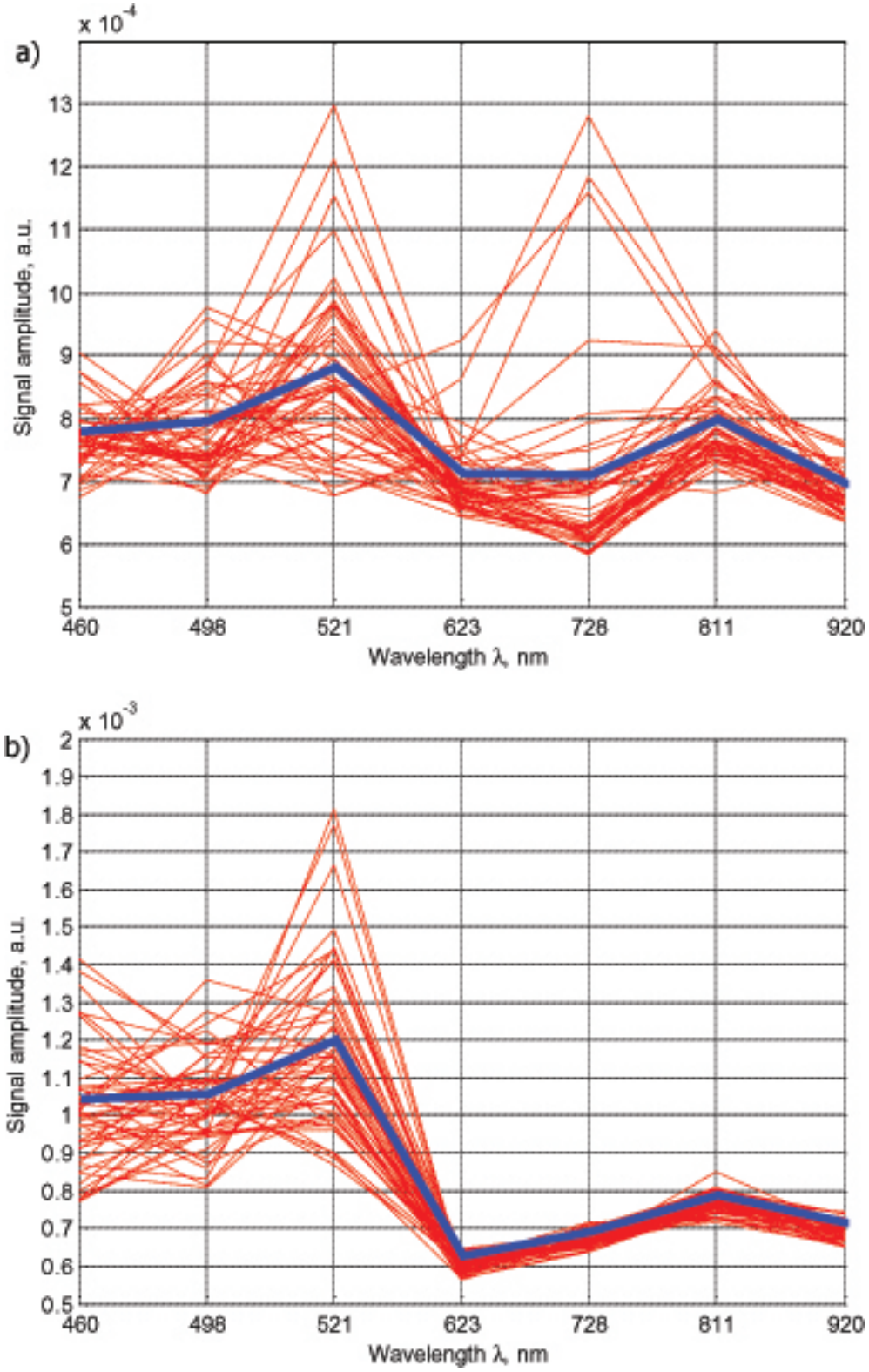

Figure 12: Average pulsation amplitude at different wavelengths for subject 1 (a) and subject 2 (b). The red lines show the average pulsation amplitudes for 50 repetitions, and the blue line their average.

7 Conclusion

We have presented an introduction to hemodynamic imaging, explaining briefly the physical and anatomical principles that are related to its operation and introducing the structure of the system along with the data analysis process for creating the results. We also introduced three existing optical medical analysis methods, photoplethysmography, pulse oximetry and laser Doppler flowmetry. Finally, we described a series of measurements and their results aimed at studying the performance of the system under different wavelengths. The experiments were conducted in accordance with the established test protocol and the analysis of the results was done using the same method as with real-life measurements with the system

The results of the experiment support the assumptions based on previous experiments conducted by our research group and existing models about the optical properties of skin, and can be used to continue developing the hemodynamic imaging system, and also to study other possible applications. One possible subject of interest is pulse oximetric imaging, which requires using the system simultaneously with two different wavelengths of illumination to create an image of the ratio of oxygenated and dexogenated blood in some area of skin. The experiments conducted in this thesis showed that all measured wavelengths produced a detectable pulsation signal which makes pulse oximetry possible. Other improvements that can be derived from these results are the selection of optimal illumination and other hardware.

The next step in improving the system is to study the relation between the amount of photons illuminating the subject and the final pulsation signal measured from them. This information could be used to clearly determine the response of both the physiological system being observed and the imaging system, which in turn would help in making separate measurements more comparable with each other and even produce quantitative measurements.

Current main focuses of the technology are migraine research, detection of arthritis-related blood perfusion disorders and skin flap blood circulation monitoring, with an even broader range of possible applications in the future. Clinical tests of the system are continuing for example in migraine research, where the system is used to detect changes in blood perfusion in the face area of migraine patients, specifically focusing on the "cold nose" symptom related with many migraine cases.

Overall, the hemodynamic imaging system is showing promise in its diagnostic capabilities, both in theory and through the clinical trials also in practice. There has been interest towards the system from various fields. In the future our aim is to continue improving the system based on the clinical tests and experiments such as those shown in this thesis.

References

[1] *Principles of Anatomy and Physiology*, 12th Edition; Tortora G.J., Derrickson B.; Wiley; Hoboken, NJ, USA, 2009

[2] *A relative color approach to color discrimination for malignant melanoma detection in dermoscopy images*; Stanley R.J., Stoecker W.V., Moss R.H.; Skin Research & Technology, Volume 13, Issue 1, p. 6272, February 2007

[3] *Pulse oximetry: its invention, theory and future*; Aoyagi T.; Journal of Anesthesia, Volume 17, p. 259-266, 2007

[4] *Analysis of transverse wave as a propagation mode for the pressure pulse in large arteries*; Lin Wang Y.Y. et al.; Journal of Applied Physics, Vol. 102, Issue 6, 2007

[5] *Photoplethysmography and its application in clinical physiological measurement*; Allen J.; Physiological measurement, Vol. 28, Issue 3, p. R1, March 2007

[6] *Uses and abuses of pulse oximetry*: Moyle J.T.B.; Archive of Diseases in Childhood, Vol. 74, p. 77-80, 1996

[7] *Feasibility of imaging photoplethysmography*; Hu S. et al.; International Conference on BioMedical Engineering and Informatics, 2008

[8] *An Imaging Pulse Oximeter Based on a Multi-Aperture Camera*; Basiri A., Ramella-Roman J.C.; IFMBE Proceedings, Vol. 32, Part 15, p. 329-331, 2010

[9] *Photoplethysmographic imaging of high spatial resolution*; Kamshilin A.A. et al.; Biomedical Optics Express, Vol. 2, No. 4, 2011

[10] *In Vivo Reflectance of Blood and Tissue as a Function of Light Wavelength*; Cui W., Ostrander L.E.; IEEE Transactions on Biomedical

Engineering, Vol. 37, No. 6, 1990

[11] *Quantitative assessment of skin layers absorption and skin reflectance spectra simulation in the visible and near-infrared spectral regions*; Meglinski I.V., Matcher S.J.; Physiological Measurement Vol. 23, p. 741-753, 2002

[12] *Structure, pattern and shape of the blood vessels of the skin*; Ryan T.J.; The Physiology and Pathophysiology of the Skin, Vol. 2, 1973

[13] *3D Multispectral Light Propagation Model For Subcutaneous Veins Imaging*; Paquit V. et al.; Medical Imaging 2008: Physics of Medical Imaging, Proceedings of SPIE, Vol. 6913, 2008

[14] *Absorption spectra and light penetration depth of normal and pathologically altered human skin*; Barun V.V. et al.; Journal of Applied Spectroscopy, Vol. 74, No. 3, 2007

[15] *Frequency-domain description of a lock-in amplifier*; Scofield J.H.; American Journal of Physics, Volume 62, Issue 2, p. 129-133, February 1994

[16] *Optics*, 4th Edition; Hecht E.; Addison Wesley; San Francisco, CA, USA, 2002

[17] *MCML - Monte Carlo modeling of light transport in multilayered tissues*; Wang L., Jacques S.L., Zheng L.; Computer Methods and Programs in Biomedicine, Vol 47, p. 131-146, 1995

[18] *Modeling optical properties of human skin using Mie theory for particles with different size distributions and refractive indices*; Bhandari A. et al.; Optics Express, Vol. 19, No. 15, 2011

[19] *Physiology, Biochemistry, and Molecular Biology of the Skin*, 2nd Edition; Goldsmith L.A.; Oxford University Press, USA, 1991

[20] *The skin: an indispensable barrier*; Proksch E., Brandner J.M., Jensen J.-M.; Experimental Dermatology, Vol. 17, p. 1063-1072, 2008

[21] *Rook's Textbook of Dermatology*, 7th Edition; McGrath J.A., Eady R.A., Pope F.M.; Blackwell Publishing, USA, 2004

[22] *The function of melanin*; Proctor P.H., McGinness J.E.; Archives of Dermatology, Vol. 122, Issue 5, 1986

[23] *Lookingbill and Marks' Principles of Dermatology*, 4th Edition; Marks J.G., Miller J.; Elsevier Inc., 2006

[24] *Clinical Dermatology*, 5th Edition; Habif T.; Mosby, 2010

[25] *Variation of Biophysical Parameters of the Skin with Age, Gender, and Body Region*; Firooz A. et al.; ScientificWorldJournal, Vol. 2012, 2012

[26] *Andrews' Diseases of the Skin: Clinical Dermatology*, 10th Edition; James W., Berger T., Elston D.; Saunders, 2005

[27] *Tissue elasticity and the ageing elastic fibre*; Sherratt M.J.; Age (Dordr), Vol. 31, Issue 4, p. 305-325, 2009

[28] *Structural and biochemical characteristics of various white adipose tissue depots*; Wronska A., Kmiec Z.; Acta Physiologica, Vol. 205, Issue 2, p. 194-208, June 2012

[29] *Method for depth-resolved quantitation of optical properties in layered media using spatially modulated quantitative spectroscopy*; Saager R.B. et al.; Journal of Biomedical Optics, Vol 16, July 2011

[30] *Reflectance spectrometry of normal and bruised human skins: experiments and modeling*; Kim O. et al.; Physilogical Measurement, Vol. 33, p.

159-175, 2012

[31] *Measurement of anisotropic reflection of flowing blood using optical coherence tomography*; Nam K.-H. at al; Journal of Biomedical Optics, Vol. 16, Issue 12, December 2011

[32] *Absorption spectra of human fetal and adult oxyhemoglobin, deoxyhemoglobin, carboxyhemoglobin, and methemoglobin*; Zijlstra W.G., Buursma A., Meeuwsen-van der Roest W.P.; Clinical Chemistry, Vol. 37, No. 9, p. 1633-1638, 1991

[33] *McDonald's Blood Flow in Arteries: Theoretical, Experimental and Clinical Principles*, 5th Edition; Nichols W.W., O'Rourke M.F.; Hodder Arnold Publication, 2005

[34] *Pulse wave analysis*; O'Rourke M.F., Pauca A., Jiang X.-J.; British Journal of Clinical Pharmacology, Vol. 51, Issue 6, p. 507-522, June 2001

[35] *Utility of the Photoplethysmogram in Circulatory Monitoring*; Reisner A. et al.; Anesthesiology, Vol. 108, Issue 5, p. 950-958, May 2008

[36] *Photoelectric plethysmography-some fundamental aspects of the reflection and transmission method*; Nijboer J.A., Dorlas J.C., Mahieu H.F.; Clinical Physics and Physiological Measurement, Vol. 2, No. 3, p. 205-215, 1981

[37] *Respiratory and non-respiratory sinus arrhythmia: implications for heart rate variability*; McMullen M.K. et al.; Journal of Clinical Monitoring and Computing, Vol. 26, p. 21-28, 2012

[38] *Development of a mobile pulsewaveform analyzer for cardiovascular health monitoring*; Bing N.L., Bin B.F., Ming C.D.; Computers in Biology and Medicine, Vol. 38, p. 438-445, 2008

[39] *Measurement of surgical stress in anaesthetized children*; Kallio H. et al.; British Journal of Anaesthesia, Vol. 101, Issue 3, 2008

[40] *Detecting Change in Left Ventricular Ejection Time During Head-Up Tilt-Induced Progressive Central Hypovolemia Using a Finger Photoplethysmographic Pulse Oximetry Wave Form*; Chan G.S.H. et al.; The Journal of Trauma, Vol. 64, p. 390-397, 2008

[41] *Two-Stage Approach for Detection and Reduction of Motion Artifacts in Photoplethysmographic Data*; Krishnan R., Natarajan N., Warren S.; IEEE Transactions on Biomedical Engineering, Vol. 57, No. 8, August 2010

[42] *Applications of Finger Photoplethysmography*; Laulkar R., Daimiwal N.; International Journal of Engineering Research and Applications, Vol. 2, Issue 1, 2012

[43] *Effects of Methemoglobinemia on Pulse Oximetry and Mixed Venous Oximetry*; Barker S.J., Tremper K.K., Hyatt J.B.S.; Anesthesiology, Vol. 70, Issue 1, p. 112-117, 1989

[44] *Confirmation of the Pulse Oximetry Gap in Carbon Monoxide Poisoning*; Bozeman W.P., Myers R.A.M., Barish R.A.; Annals of Emergency Medicine, Vol. 30, Issue 5, 1997

[45] *Frequency-domain description of a lock-in amplifier*; Scofield J.H.; American Journal of Physics, Vol. 62, Issue 2, 1994

[46] *Detection of Small and Noisy Signals in Sensor Interfacing: The Analog Lock-in Amplifier*; De Marcellis A., Ferri G.; Analog Circuits and Signal Processing, Analog Circuits and Systems for Voltage-Mode and Current-Mode Sensor Interfacing Applications, p. 181-204, 2011

[47] *High-performance modular digital lock-in amplifier*; Barone F. et al; Review of Scientific Instruments, Vol. 66, No. 6, June 1995

[48] *A modular, low-cost, digital signal processor-based lock-in card for measuring optical attenuation*; Barragan L.A., Artigas J.I.; Review of Scientific Instruments, Vol. 72, No. 1, January 2001

[49] *The Optics of Human Skin*; Anderson R.R., Parrish J.A.; The Journal of Investigative Dermatology, Vol 77, No. 1, 1981

[50] *Near-infrared optical properties of ex vivo human skin and subcutaneous tissues measured using the Monte Carlo inversion technique*; Simpson C.R. et al.; Physics in Medicine and Biology, Vol. 43, p. 2465-2478, 1998

[51] *Ultrastructure of the human dermal microcirculation: The horizontal plexus of the papillary dermis*; Yen A., Braverman I.M.; The Journal of Investigative Dermatology, Vol. 66, p. 131-142, 1972

[52] *Optical properties of human skin, subcutaneous and mucous tissues in the wavelength range from 400 to 2000nm*; Bashkatov A.N. et al.; Journal of Physics D: Applied Physics, Vol. 38, p. 2543-2555, 2005

[53] *Absorption and attenuation of visible and near-infrared light in water: dependence on temperature and salinity*; Pegau W.S., Gray D., Zanevald R.V.; Applied Optics, Vol. 36, No. 24, 1997

[54] *A New Instrument for Continuous Measurement of Tissue Blood Flow by Light Beating Spectroscopy*; Nilsson G.E., Tenland T., Öberg P.Å.; IEEE Transactions on Biomedical Engineering, Vol 27, No. 1, 1980

[55] *Evaluation of a Laser Doppler Flowmeter for Measurement of Tissue Blood Flow*; Nilsson G.E., Tenland T., Öberg P.Å.; IEEE Transactions on Biomedical Engineering, Vol 27, No. 10, 1980

[56] *Model for laser Doppler measurements of blood flow in tissue*; Bonner R., Nossal R.; Applied Optics, Vol. 20, No. 12, 1981